

## **Design and implementation of Hexa-triangular antenna for UWB wireless communication**

<sup>1</sup>N.Porcherlvi, <sup>2</sup>R.Dhanya, <sup>3</sup>V.Priyalakshmi

*Department of Electric and Electronic Engineering, Vivekanandha College Of Technology For Women, Thiruchengodu, Namakkal.*

**Abstract:** A modified hexagonal Sierpinski gasket-based fractal antenna is proposed for ultrawide-band (UWB) wireless applications. The designed antenna has miniaturized ( $36.48 \text{ mm}^2$ ) and multiband characteristics. Two design guidelines, the partial ground plane technique and the circular annular ring patch on the substrate, are applied to improve impedance matching and radiation pattern characteristics. According to the simulation results, the proposed modified antenna has a reflection coefficient  $S_{11}$  of less than  $\{-15 \text{ dB}$ , a linear phase of the reflection coefficient, 80% radiation efficiency,  $2\{4.5 \text{ dBi}$  antenna gain, and omnidirectional radiation pattern properties over the full UWB spectrum ( $3.1\{10.6 \text{ GHz}$ ). Simulated results obtained for this antenna show the expected good radiation behavior within the full 7.5-GHz UWB bandwidth.

**Key words:** Ultrawide-band antenna, Sierpinski gasket, miniaturized, multiband

---

### **I. Introduction**

Rising bandwidth demands of wireless network subscribers due to the growth of high-quality multimedia services such as video conferencing and home video sharing push the wireless access network designs towards new alternative technologies. Ultrawide-band (UWB) signaling methodology has some unique characteristics for use in short-range wireless communication systems, which bring new opportunities for wireless coverage areas. UWB technology has some strong intrinsic features such as low self-interference, multipath immunity, minimal interference, and penetration through obstacles while preserving link integrity [1]. This technology has some state-of-the-art transmission characteristics such as ultrahigh bandwidths with noise-like power levels in a typical indoor environment (FCC part 15:  $\{-41.3 \text{ dBm/MHz}$ ) [2]. In the future, UWB systems are expected to operate in the entire UWB spectrum ( $3.1\{10.6 \text{ GHz}$ ). Multiband orthogonal frequency division multiplexing (MB-OFDM) is an attractive modulation technique for multiuser UWB communication due to multipath energy efficiency, low interference between subcarriers, and high spectral efficiency [3]. Therefore, MB-OFDM based on UWB signaling methodology is projected to enhance a new perspective for high-definition video communication in wireless personal area networks [4]. One of the challenging research objectives is to propose miniaturized, cost-effective antennas with power radiation uniformly in all transmission directions, ultrahigh bandwidth, and nondispersive behavior for UWB communication systems [5]. The antenna model is also critical since it has a major impact on the complexity and size of the receiver and transmitter designs for portable devices [6].

It was determined that planar monopoles offer compact, broadband, and omnidirectional characteristics for antenna designs [7]. Accordingly, several planar monopoles with different geometries have been proposed and experimentally characterized for wide-band applications [8{10]. Self-similarity and space-filling features are two well-known methodologies for achieving multiband and miniaturized characteristics for antenna designs [11].

Fractal geometries show key intrinsic properties as compared with traditional Euclidian ones, such as self-similarity, space-filling, and self-avoiding properties [12]. The space-filling characteristic could enhance the power transfer from the antenna design to the transmission medium (usually air) by utilizing smaller spaces. Consequently, miniaturization and operation on a desired frequency spectrum could be achieved.

There are several well-known fractal geometries for antenna applications in the literature that ensure small sizes and multiband characteristics, including the Hilbert fractal, Koch, Sierpinski gasket, Pythagorean tree, and Giusepe Peano designs [13{17]. In the current paper, the Sierpinski gasket (also known as the Sierpinski triangle) was chosen as a fractal geometry for antenna design since the design has a similarity to the well-known triangular concept. A fractal antenna is proposed in this paper in order to utilize the complete UWB spectrum ( $3.1\{10.6 \text{ GHz}$ ) by introducing the hexagonal fractal structure formed by using six copies of the second-iteration triangular Sierpinski gasket. The mathematical generation of the hexagonal Sierpinski gasket is presented in the first section by inheriting the center of masses of the subtracted triangles. The antenna reflection coefficient, gain, and radiation performance characteristics are shown in the second section. The proposed

antenna has good transmission characteristics with acceptable reflection coefficients, omnidirectional radiation patterns, and promising efficiency.

## II. Antenna design

### 2.1. The ideal Sierpinski fractal concept

The Sierpinski gasket, or Sierpinski triangle, is a very popular fractal structure that was described by the Polish mathematician Waclaw Sierpinski in 1915 [18]. A self-similar current distribution that generates multiband behaviors for antenna designs is produced. The multiband characterization of the Sierpinski fractal antenna has been investigated and it was discovered that the perturbing of this fractal geometry can be used as a control technique for multiband behavior [19{22]. Furthermore, a Sierpinski gasket fractal-based antenna and closed-form mathematical calculations were proposed in [23]. A Sierpinski triangle is generated using a technique known as the iterative function system (IFS). The generation process of the proposed hexagonal Sierpinski-based monopole antenna is depicted in Figure 1.

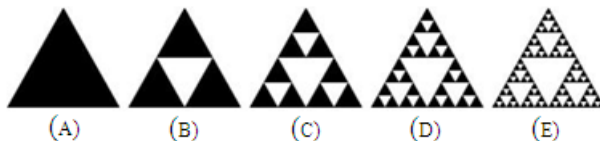


**Figure 1.** Sierpinski gasket generation process: (a) initiator, (b) 1st iteration, (c) 2nd iteration, (d) 3rd iteration, (e) 4th iteration.

The initiator (Figure 1a) is an inverted equilateral triangle; the equilateral nature allows for scaling symmetry and would also result in easy segment bisection. An equilateral triangle that is half the size (both width and height) of the main triangle is subtracted from the initiator to form the first iteration of the Sierpinski gasket geometry, as depicted in Figure 1b. The subtraction is arranged in such a way that three equal-sized, equilateral triangles are generated. The edge of each newly generated triangle touches the other two triangles at a corner.

Figure 1b illustrates that the first iteration generates a triangular hole in the middle of the main triangle shape. This is a result of the scaled-down triangles only taking 3 parts of the 4 part geometry, resulting in one remaining part un filled (a triangular hole). For the later iterations, the same subtraction procedure continues for the remaining triangles, as seen in Figures 1c, 1d, and 1e. When closely analyzed, it can be noticed that the Sierpinski set is a variant form of the repetitive structures that are said to be self-similar. The geometric construction of the Sierpinski fractal and the centric points of the subtracted triangles are depicted in Figure 2.

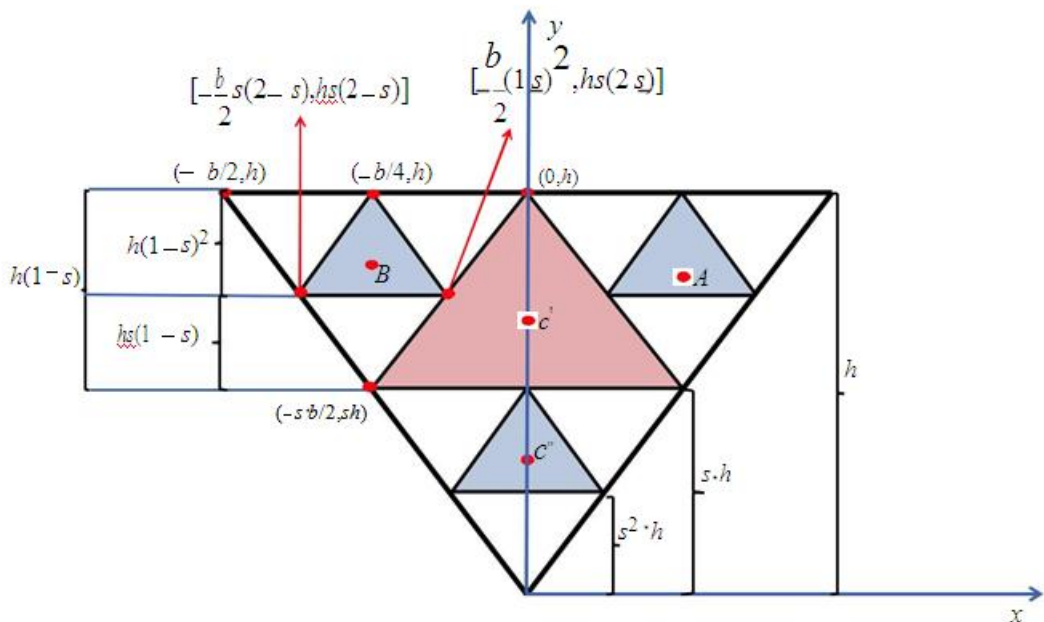


**Figure 2.** Mathematical representation for the generation of the 2nd iteration Sierpinski gasket.

The center of the main triangle shape, the initiator, is defined as  $c = (0; h=3)$ . Mathematical representations are characterized in a general manner so that the perturbations on Sierpinski fractal structures can also be analyzed. In the proposed triangle, the two side lengths of the upside-down triangle are assumed to be  $a$  and the

top side is  $b$ . Mathematical representations are obtained in the case that  $b \neq a$ . On the other hand, the scaling factor ( $s$ ) is defined as 0.5 for ideal structures where  $b = a$  as the side length of an equilateral triangle.

For later iterations, the center of the subtracted triangles from the first iteration ( $c'$ ) and the second iteration ( $c''$ ) are  $A$  and  $B$ : The coordinates of these centric points are defined as follows:

$$X = \frac{x_1 + x_2 + x_3}{3}; \quad (1)$$

$$Y = \frac{y_1 + y_2 + y_3}{3}. \quad (2)$$

From the above equations, we obtain:

$$c' = \left[ \begin{array}{c} \frac{1}{3} \\ 0; sh + 3h(1-s) \end{array} \right]; \text{ for } s = \frac{1}{2}; c' = \left[ \begin{array}{c} \frac{1}{3} \\ 0; 3 \end{array} \right]; \quad (3)$$

$$\frac{1}{3} \quad \frac{1}{3} \quad \frac{h}{3} \quad (4)$$

$$c'' = \left[ \begin{array}{c} 0; s^2h + 3sh(1-s) \end{array} \right]; \text{ for } s = \frac{1}{2}; c'' = \left[ \begin{array}{c} 0; 3 \end{array} \right];$$

$$A = \left[ \begin{array}{c} \frac{b}{4}; \frac{h + 2sh(2-s)}{3} \end{array} \right]; \text{ for } s = \frac{1}{2}; A = \left[ \begin{array}{c} \frac{b}{4}; \frac{5h}{6} \end{array} \right]; \quad (5)$$

$$B = \left[ \begin{array}{c} \frac{b}{4}; \frac{h + 2sh(2-s)}{3} \end{array} \right]; \text{ for } s = \frac{1}{2}; B = \left[ \begin{array}{c} \frac{b}{4}; \frac{5h}{6} \end{array} \right]; \quad (6)$$

Dimensioning is a quite important terminology for fractal-based antennas in terms of size definition. It can be described in several ways, but the simplest and best known one is the self-similarity dimension [24]. The self-similarity dimension for the Sierpinski gasket is shown below.

$$D = \frac{\log n}{\log \frac{1}{s}} \quad (7)$$

The number of copies of the initiator is specified with the parameter  $n$  and the geometry scaled-down fraction ( $s$ ) is defined as 0.5 for the ideal Sierpinski gasket.

## 2.2. A modified hexagonal Sierpinski fractal antenna

The proposed modified hexagonal Sierpinski gasket antenna preserves most of the generation stages of the original Sierpinski fractal concept. Figure 3 shows the generation stages and the ultimate modified Sierpinski gasket. The generation process is exactly the same as the ideal Sierpinski gasket, with an equilateral triangle and a scaling factor ( $s = 0.5$ ) up to the second iteration. This can be seen in Figures 3a, 3b, and 3c. The final geometry is truncated after combining the six copies of the second iteration in a way that resembles a hexagonal structure, as shown in Figure 3d.

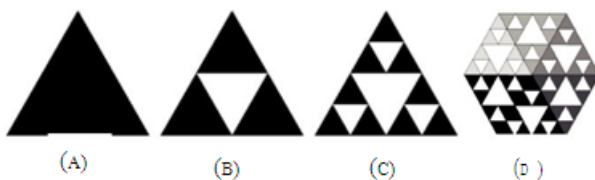


**Figure 3.** Proposed modified Sierpinski gasket antenna: (a) initiator, (b) 1st iteration, (c) 2nd iteration, (d) hexagonal Sierpinski gasket.

The hexagonal Sierpinski gasket fractal-based monopole antenna configuration is shown in Figure 4. The antenna was constructed on a Roger RO4232 substrate with a thickness of 1.45 mm, a relative dielectric constant ' $\epsilon_r$ ' of 3.2 and 0.0018 dielectric loss tangent, and a size of 36.48 mm (width height).

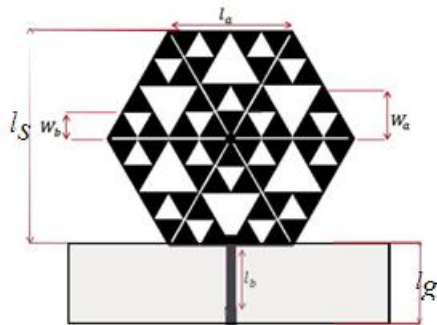


**Figure 4.** Dimensioning of the hexagonal Sierpinski fractal-based antenna structure.

The dimensions of the configuration are as follows:  $l_s = 24.4$  mm,  $l_a = 14.2$  mm,  $w_a = 7$  mm,  $w_b = 3.5$  mm, and  $l_b = 10.2$  mm. A microstrip line with a feeding section is formed for the feeding section of the proposed antenna [25]. A modified ground plane is applied on the dielectric substrate with a  $50\text{-}\Omega$  microstrip feed line in order to achieve ultrahigh bandwidth with omnidirectional radiation characteristics.

### III. Results and discussion

The proposed modified hexagonal Sierpinski fractal was generated with commercially available Ansoft HFSS software and simulated using the finite element method. An absorbing boundary condition environment was used to simulate in an open-domain transmission medium. The adaptive meshing technique was applied for the proposed simulation model (HFSS). The adaptation frequency was 6.9 GHz since it is a close value to the center of the full UWB spectrum (3.1{10.6 GHz). It was also observed that additional discrete frequency points improved field performances for higher frequencies (above 9 GHz). Consequently, a further frequency sweep was applied at 10.3 GHz to achieve improved simulation results. As a first research challenge, the proposed microstrip monopole antenna performance was studied with various ground plane lengths ( $l_g$ ). The simulated return loss ( $S_{11}$ ) curves with different values of  $l_g$  for the hexagonal Sierpinski antenna over the 3.1{10.6 GHz UWB range are shown in Figure 5.

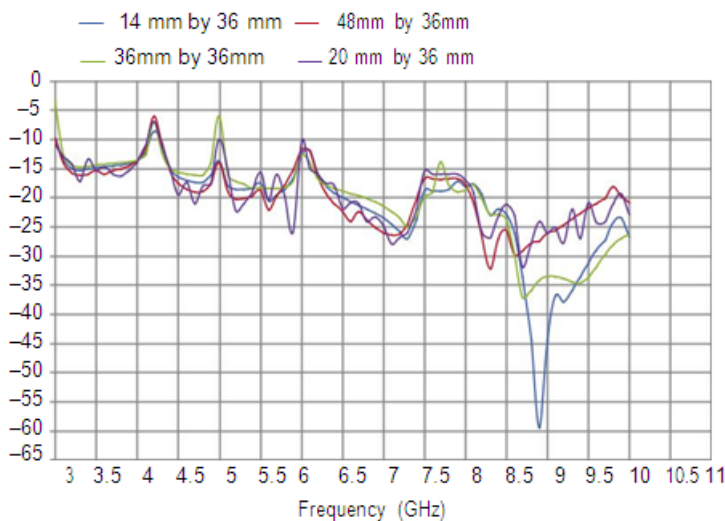


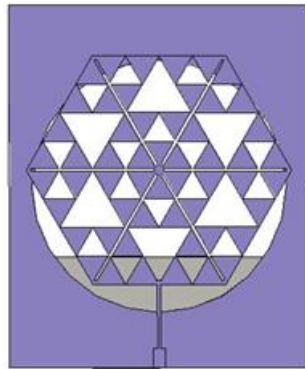
**Figure 5.** Simulated reflection coefficients of the proposed hexagonal Sierpinski antenna with different values of  $l_g$ .

The impedance bandwidth could be further enhanced by applying different sizes of ground plane lengths, as shown in Figure 5. Values that were smaller than 14 mm had a minimal effect on impedance bandwidth. Therefore, the optimized value of  $l_g$  was chosen as 14 mm. For further antenna matching improvements the circular annular patch technique was applied to the substrate [26].

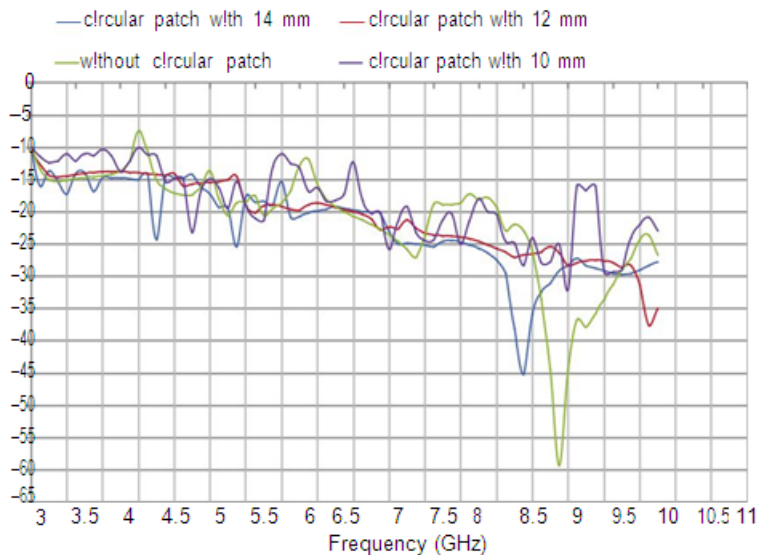
The modified hexagonal Sierpinski fractal-based monopole antenna picture with a circular ring patch is illustrated in Figure 6. The ring laceration on the substrate performs as an air dielectric that enhances the

reduction of surface wave excitation. With this technique, the electric field could be increased without changing the physical size of the antenna. Accordingly, the input resistance of the antenna is improved for the proposed frequency range while keeping it compact.

The simulated return loss ( $S_{11}$ ) curves with various circular ring patches for the proposed antenna over the UWB spectrum (3.1–10.6 GHz) are shown in Figure 7.



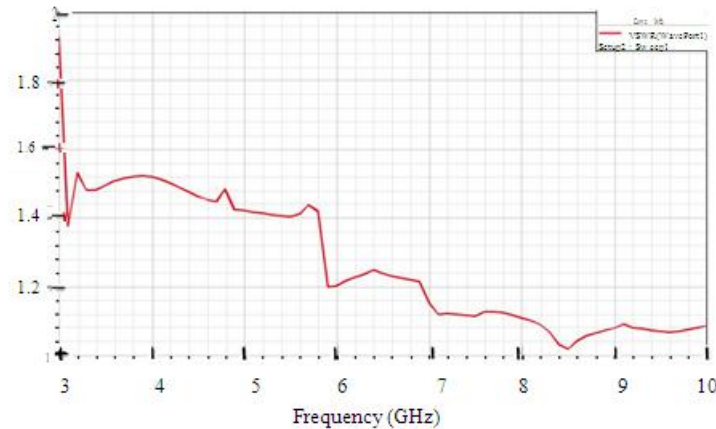
**Figure 6.** A picture of the proposed hexagonal Sierpinski fractal-based monopole antenna with a circular ring patch.



**Figure 7.** Simulated reflection coefficient versus frequency with different values of circular patch.

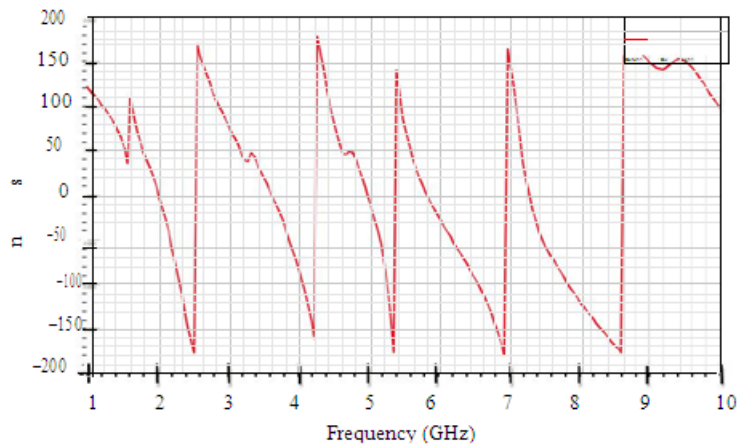
After simulating for different sizes of circular patches, it was observed that impedance bandwidth and radiation characteristics were improved. It was also realized that for all simulated sizes of the annular rings,  $S_{11}$  results were below  $\{-10\text{ dB}$  for the full UWB bandwidth. The optimized value for the circular patch was chosen as 14 mm.

It is well known that  $S_{11}$  below  $\{-10\text{ dB}$  is satisfactory for UWB transmission. The proposed antenna showed effective matching properties with  $S_{11}$  below  $\{-15\text{ dB}$ . The rest of the simulation analysis was carried out by considering the optimized  $l_g$  and circular patch on the proposed hexagonal Sierpinski antenna. Figure 8 illustrates the simulated results of the voltage standing wave ratio (VSWR) for the proposed antenna. It can be observed that simulated VSWR readings are less than 1.5, implying an expected performance when considering return loss results.



**Figure 8.** VSWR simulation results.

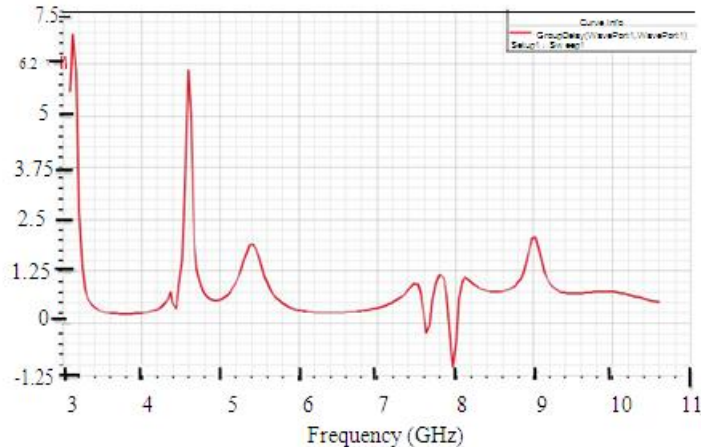
The plots in Figures 7 and 8 indicate that the antenna is matched and the input current is transmitted by the antenna. In UWB systems, it is quite crucial to achieve a linear phase response of the radiated field and a stable group delay response over the full UWB spectrum. These characteristics enhance minimal distortion for the radiated pulse. As illustrated in Figure 9, the phase plot of the proposed antenna shows almost linear characteristics for the full UWB spectrum. Accordingly, the antenna group delay shows a persistent behavior over the 3.1{10.6 GHz range, as shown in Figure 10, which indicates a nondistorted time domain response of the proposed antenna design.



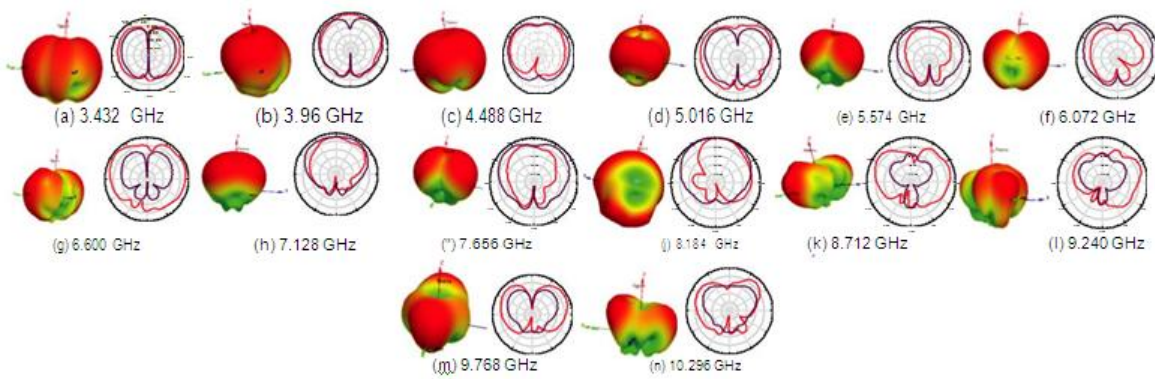
**Figure 9.** The phase of the reflection coefficient versus frequency for the proposed antenna.

Figure 11 illustrates the simulated two- and three-dimensional radiation patterns of the proposed antenna at various frequencies through the UWB bandwidth (3.1{10.6 GHz). The behavior of the E-plane and the H-plane of the proposed antenna is indicated by the purple and red lines, respectively, at various frequencies.

It can be observed from Figures 11a{11n that all of the patterns are omnidirectional and provide spherical coverage with stable radiation patterns over the full UWB range (3.1{10.6 GHz). At 10 GHz and above, however, the antenna is expected to experience losses in gain and range; this can be ascribed to limitations in the substrate and higher mode excitation by the structure. Most of the patterns have an '8'-shaped pattern corresponding to a 3D pattern with a toroidal shape. The simulated patterns are expected due to the characteristics of the printed monopole. The antenna gain versus frequency is depicted in Figure 12, showing a satisfactory antenna gain in the UWB range. There is a slight increase observed at higher frequencies as a result of the directional patterns.



**Figure 10.** Group delay for the modified hexagonal Sierpinski gasket.



**Figure 11.** Radiation patterns of the proposed antenna over the UWB bandwidth (3.1{10.6 GHz).

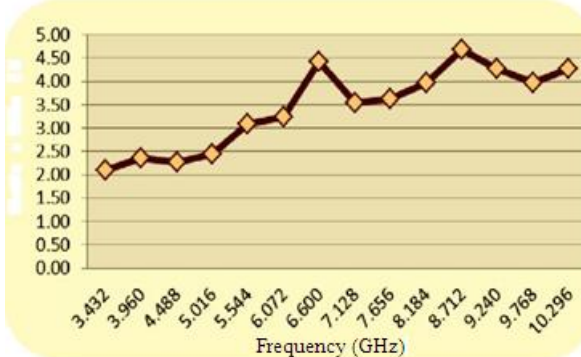


**Figure 12.** Antenna gain over UWB bandwidth.

#### IV. Conclusions

A miniaturized ( $36.48 \text{ mm}^2$ ) antenna design is proposed by utilizing the space-filling and self-similarity properties of fractal geometries. The antenna is based on hexagonal Sierpinski fractal geometry and has multiband, broadband, and good electrical characteristics. The proposed antenna is characterized for the complete UWB spectrum (3.1{10.6 GHz). Better antenna characteristics are achieved by applying the partial ground plane technique and inserting a circular patch to the substrate. Based on the results, we can conclude that there is a matched impedance bandwidth in the full-band UWB range with desired reflection coefficient characteristics (better than {15 dB). In line with these characteristics, the proposed antenna has 80% radiation efficiency over the full UWB bandwidth. The radiation patterns show omnidirectional transmission performances. The proposed miniaturized hexagonal Sierpinski-based fractal antenna demonstrates efficient performance results that can be used for UWB communication.

## References

- [1]. Kohno R. State of arts in ultra wideband (UWB) wireless technology and global harmonization. In: IEEE 2004 European Microwave Conference; 12{14 October 2004; Amsterdam, the Netherlands. New York, NY, USA: IEEE. pp. 1093{1099.
- [2]. FCC. Revision of Part 15 of the Commission's Rules Regarding Ultra-Wideband Transmission Systems FCC, Report FCC 02{48. Washington, DC, USA: FCC, 2002.
- [3]. Balakrishnan J, Batra A, Dabak A. A multi-band OFDM system for UWB communication. In: IEEE 2003 Ultra Wideband Systems and Technologies Conference; 16{19 November 2003; Reston, VA, USA. New York, NY, USA: IEEE. pp. 354{358.
- [4]. Duan C, Pekhteryev G, Fang J, Nakache Y, Zhang J, Tajima K, Nishioka Y, Hirai H. Transmitting multiple HD video streams over UWB links. In: IEEE 2006 Consumer Communications and Networking Conference; 8{10 January 2006; Las Vegas, NV, USA. New York, NY, USA: IEEE. pp. 691{695.
- [5]. Schantz H. The Art and Science of Ultrawideband Antennas. 1st ed. Norwood, MA, USA: Artech House, 2005.
- [6]. Chen NZ, Wu XH, Li HF, Yang N, Chia MYW. Considerations for source pulses and antennas in UWB systems. IEEE T Antenn Propag 2004; 7: 1739{1748.
- [7]. Agrawall NP, Kumar G, Ray KP. Wideband planar monopole antennas. IEEE T Antenn Propag 1998; 46: 294{295.
- [8]. Low ZN, Cheong JH, Law CL. Low-cost PCB antenna for UWB applications. IEEE Antenn Wirel Pr 2005; 4: 237{239.
- [9]. Suh SY, Stutzman WL, Davis WA. A new ultrawideband printed monopole antenna: the planar inverted cone antenna (PICA). IEEE T Antenn Propag 2004; 52: 1361{1364.
- [10]. Jung J, Choi W, Choi J. A small wideband microstrip fed monopole antenna. IEEE Microw Lett 2005; 15: 703{705.
- [11]. Hansen CR. Fundamental limitations in antennas. P IEEE 1981; 69: 170{182.
- [12]. Werner DH, Ganguly S. An overview of fractal antennas engineering research. IEEE Antenn Propag M 2003; 45: 38{56.
- [13]. Hwang KC. A modi ed Sierpinski fractal antenna for multiband application. IEEE Antenn Wirel Pr 2007; 6: 357{360.
- [14]. Pourahmazdar J, Ghobadi C, Nourinia J. Novel modi ed Pythagorean tree fractal monopole antennas for UWB applications. IEEE Antenn Wirel Pr 2011; 10: 484{487.
- [15]. Oraizi H, Hedayati S. Miniaturized UWB monopole microstrip antenna design by the combination of Giusepe Peano and Sierpinski carpet fractals. IEEE Antenn Wirel Pr 2011; 10: 67{70.
- [16]. Kaka AO, Toycan M, Bashiry V, Walker SD. Modi ed Hilbert fractal geometry, multi-service, miniaturized patch antenna for UWB wireless communication. COMPEL 2012; 31: 1835{1849.
- [17]. Sundaram A, Maddela M, Ramadoss R. Koch-Fractal folded-slot antenna characteristics. IEEE Antenn Wirel Pr 2007; 6: 219{222.
- [18]. Peitgen HO, Jurgens H, Saupe D. Chaos and Fractals. 2nd ed. New York, NY, USA: Springer-Verlag, 2004.
- [19]. Puente C, Romeu J, Pous R, Garcia X, Benitez F. Fractal multiband antenna based on the Sierpinski gasket. IEEE Elect Lett 1996; 32: 1{2.
- [20]. Puente C, Romeu J, Bartolome R, Pous R. Perturbation of the Sierpinski antenna to allocate operating bands. IEEE Elect Lett 1996; 32: 2186{2188.
- [21]. Puente C, Romeu J, Pous R, Cardama A. On the behavior of the Sierpinski multiband fractal antenna. IEEE T Antenn Propag 1998; 46: 517{524.
- [22]. Kaka A, Toycan M, Bashiry V, Ademgil H, Walker SD. A fractal geometry, multi-band, miniaturized monopole antenna design for UWB wireless applications. In: IEEE-APS 2011 Antennas and Propagation in Wireless Communication Topical Conference; 12{16 September 2011; Turin, Italy. New York, NY, USA: IEEE. pp. 584{587.
- [23]. Mishra RK, Ghatak R, Poddar DR. Design formula for Sierpinski gasket pre-fractal planar-monopole antennas. IEEE Antenn Propag M 2008; 50: 104{107.
- [24]. Vinoy KJ, Abraham JK, Varadan VK. On the relationship between fractal dimension and the performance of multi-resonant dipole antennas using Koch curves. IEEE T Antenn Propag 2003; 51: 2296{2303.
- [25]. Kimouche H, Abed D, Atrouz B, Aksas R. Bandwidth enhancement of rectangular monopole antenna using modi ed semi-elliptical ground plane and slots. Microw Opt Techn Let 2010; 52: 54{58.
- [26]. Nikolic MM, Djordjevic AR. Improving radiation pattern of microstrip antennas. In: IEEE 2006 Antennas and Propagation Conference; 6{10 November 2006; Nice, France. New York, NY, USA: IEEE. pp. 1{6.